USDA UNITED STATES DEPARTMENT OF AGRICULTURE

Agricultural Research Service

National Sedimentation Laboratory
Oxford, Mississippi 38655

Sedimentation Patterns within a Flood Control Reservoir: Grenada Lake, MS

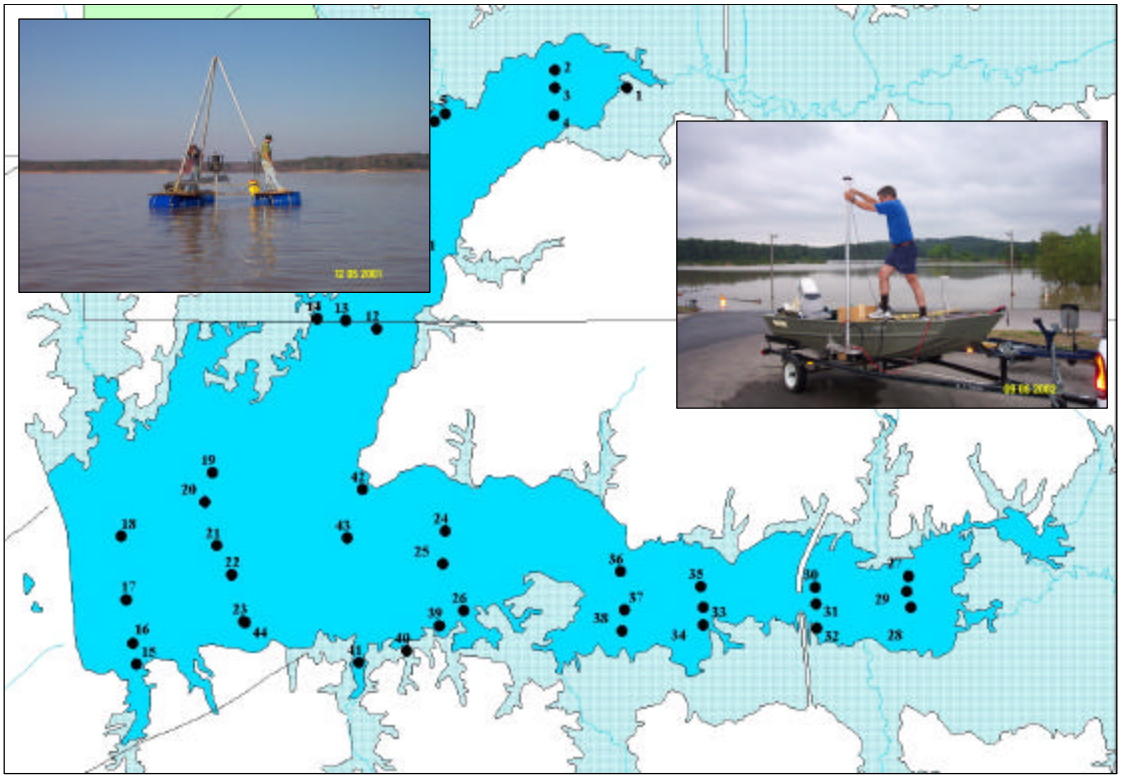

By John A. Dunbar, Sean J. Bennett, Paul D. Higley, and Fred E. Rhoton

Research Report No. 38 **April 2003**

EXECUTIVE SUMMARY

Streams in the Yalobusha River basin of north-central Mississippi have experienced severe erosion, bed incision, and channel widening due to channelization projects during the early 1900s and again in the 1950s and 1960s. Straightening of the Yalobusha River and Topashaw Creek has markedly altered the base level of these streams and promoted basin-wide degradation of the river channels. Changes in base level caused channel incision, bank destabilization, and channel widening. As a result, large volumes of sediment and woody riparian vegetation were delivered to the flow and subsequently transported through the river network. At the point where the channelized, straightened Yalobusha River met the natural, unchannelized meanders downstream, the woody debris in transport were deposited. These processes, left unrequited for decades, resulted in the rapid and progressive accumulation of a large woody debris plug on the lower Yalobusha River downstream of Calhoun City, MS. This debris accumulation has significantly increased the magnitude, frequency, and severity of flooding in the Calhoun City area. Before the U.S. Army Corps of Engineers initiates debris plug removal and channel improvements, an assessment of sedimentation within Grenada Lake located downstream of the plug is required. This report summarizes research data collected to meet this need.

Forty-seven continuous sediment cores, ranging in length from 0.55 to 2.55 m, were collected within Grenada Lake. Select cores were analyzed for particle size, agrichemicals, bulk sediment chemistry, bulk density, total carbon, and isotopes (reported in Bennett and Rhoton, 2003). Discrimination of post-impoundment sediment (sediment deposited since dam construction) and pre-impoundment sediment (parent material or pre-existing sediment) was accomplished by the use of chemical isotopes and variations in sediment texture and bulk density with depth.

A multi-frequency acoustic profiling system was used to image the post-impoundment sediment below the bottom of the lake. Using the results of the stratigraphic analysis, there is very good agreement between the acoustically-determined impoundment horizons and the stratigraphically-determined sediment thicknesses. Sediment tends to be thicker in the topographic lows, or in this case the relict or drowned Yalobusha and Skuna River channels, as compared to the plateaus on either side representing the relict floodplains. Although there are small pockets of very thick sediment, >2 m, the impounded sediment in the arms of the Yalobusha and Skuna Rivers is about 0.5 to 1.0 m thick and about 1.5 m thick in the main pool of the lake. Sediment thickness tends to increase towards the pool region.

The total volume of accumulated sediment based on these results is 40,357 ac-ft (49,790,128 m^3), assuming that sediment thickness is zero at the lake shoreline. The as-built flood control storage is 1,251,710 ac-ft at a pool elevation of 231 ft. Using these values, the loss of flood control storage due to reservoir sedimentation since dam construction is approximately 3.3%. Thus, the reservoir has an annual storage loss of about 0.1%. These accumulation rates do not include sedimentation within the tributaries upstream of the lake and are restricted in space to those areas surveyed.

TABLE OF CONTENTS

LIST OF ILLUSTRATIONS

LIST OF TABLES

ACKNOWLEDGEMENTS

We gratefully acknowledge the technical assistance of Glenn Gray, Vince Cambell, Dan McChesney, Will Beard, Corey Patrick, and Collin Anderson. Financial and programmatic support was provided by Mr. Thomas L. Hengst, Senior Project Manager, Demonstration Erosion Control Project, U.S. Army Corps of Engineers (COE), Vicksburg District, MS.

Author contact information:

John A. Dunbar, Department of Geology, Baylor University, P.O. Box 97354, Waco, TX 76798-7354, john_dunbar@baylor.edu

Sean J. Bennett, USDA-ARS National Sedimentation Laboratory, P.O. Box 1157, Oxford, MS 38655, sjbennett@ars.usda.gov

Paul D. Higley, Specialty Devices, Inc., 1104 Summit Avenue, Suite #104, Plano, TX 75074, sdipdh@aol.com

Fred E. Rhoton, USDA-ARS National Sedimentation Laboratory, P.O. Box 1157, Oxford, MS 38655, frhoton@ars.usda.gov

1. INTRODUCTION

1.1 Background

A large number of stream channels in the Midwestern United States have been subjected to severe erosion and incision due to channelization programs during the early 1900s and again in the 1950s and 1960s (Simon and Rinaldi, 2000). These erosional processes, caused in many cases by migrating knickpoints several meters in height, were exacerbated by the low cohesive strength of the loess-derived soils. The streams within the Yalobusha River basin, located in north-central Mississippi within the bluff hills region of the state, have also experienced severe erosion, bed incision, and channel widening (Simon, 1998). Straightening of the Yalobusha River and Topashaw Creek, most recently as 1967, has markedly altered the base level of these streams and promoted basin-wide degradation of the river channels.

The primary results of changing base level within the Yalobusha River basin are channel incision, bank destabilization, and channel widening (Simon and Thomas, 2002). Large volumes of sediment and woody riparian vegetation were delivered to the flow and were transported through the river network (Downs and Simon, 2001). When the channelized, straightened Yalobusha River reaches met the natural, unchannelized meanders, the woody debris in transport would become snagged and deposited. These processes, left unrequited for decades, resulted in the rapid accumulation of a large woody debris plug on the lower Yalobusha River downstream of Calhoun City, MS. This is the third known debris accumulation in the last 60 years. Estimates by Simon (1998) and Downs and Simon (2001) suggest that as much as 5 m of sediment and debris has accumulated vertically since 1967 and input of vegetation due to bank failure in the vicinity of major knickpoints is around 28 m^3/yr. This debris accumulation has significantly increased the magnitude, frequency, and severity of flooding in the Calhoun City area.

1.2 Problem Statement

Before the Corps of Engineers, Vicksburg District, initiates debris plug removal and channel improvements, an assessment of sedimentation within Grenada Lake located downstream of the plug is required. To meet this need, the following work was proposed (January, 2002).

1. Samples of the sediment trapped within Grenada Lake will be collected using vibracoring and acoustic technology.
2. All sediment samples will be analyzed for particle size and bulk density, historical agrichemicals, and heavy metals and chemical elements.
3. The primary deliverable is a report summarizing sediment thickness, stratigraphy, and chemical and physical characteristics of the sediment impounded within Grenada Lake.

This report summarizes the main findings of the field data collection program within Grenada Lake to map the distribution of impounded sediment, or sediment deposited since the dam was constructed, using acoustic profiling technology. Descriptions of the methods and procedures as well as sample locations are also presented and discussed. The physical and chemical characteristics of the sediment have been presented elsewhere (Bennett and Rhoton, 2003).

2. PROCEDURES

2.1 Sediment Coring

A commercially available vibracoring system was used to core sediments within Grenada Lake (Figures 2-1 to 2-4). Vibracoring is a common approach for obtaining undisturbed cores of unconsolidated sediment in saturated or nearly saturated conditions (Lanesky et al., 1979; Smith, 1984). This system uses a 1-HP motor that drives a pair of weights (masses) eccentrically mounted on two shafts, and it is housed within a watertight aluminum chamber so it can be immersed in water (Figure 2-1). The chamber (driver) was connected to the top of an aluminum irrigation pipe 1.5-mm in thickness and 76-mm in diameter that was cabled to a 4.2-m high aluminum tripod fitted with a battery-operated winch. The driver is equipped with a 50-ft power cord, thus limiting the depth of operation. Lengths of core pipe 4-m long were used, although longer lengths are possible. The tripod was mounted to a raft that could be easily carried and assembled on site, towed with a small boat, and anchored into position (Figures 2-1 to 2-4).

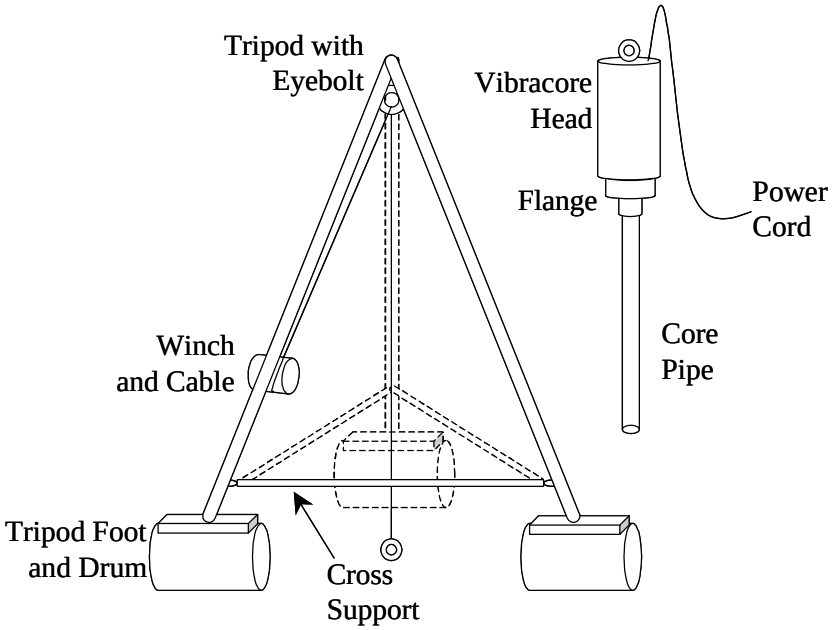

Figure 2-1. Schematic diagram of vibracoring system.

Figure 2-2. Picture of vibracorer taken on Grenada Lake.

Figure 2-3. Picture of the vibracorer taken during operation on the Yalobusha River. Core pipe is fully extended.

Figure 2-4. Picture of the vibracorer taken during operation on Grenada Lake. Core pipe is being pulled from the lake.

2.2 Acoustic Profiling System

The acoustic profiling system used herein was developed in a collaboration between Baylor University and Specialty Devices, Inc. Plano, TX (SDI; Dunbar, et al., 1999; Figures 2-5 and 2-6). The system was designed for sediment surveys of large water supply reservoirs, but it also has been used to survey lakes, harbors, and rivers. In the commercialized version used in the Grenada Lake survey, the electronics module includes a built-in computer that controls the acoustic profiling and navigation, a computer monitor, and a differential GPS navigation system. All of these components are contained in one, suitcase-sized water-resistant box (Figure 2-5). The electronics module weighs 12 kg. Power for the electronics module and acoustic source is supplied by one 12-volt marine battery.

The system images the bottom and sub-bottom with multiple, widely separated acoustic frequencies at a time. Versions of the SDI system are available with up to five signal frequencies. During acquisition, the system collects traces using each transducer independently in rapid, round-robin succession. The high-frequency signals provide a sharp image of low-density fluid mud at the water bottom, whereas the low-frequency signals penetrate many meters of the subsurface to image the base of sediment fill. For the Grenada Lake survey a three-frequency system was used, with acoustic transducers with central frequencies of 200, 48, and 24 kHz (Figure 2-6). Generally, the best image of the pre-impoundment surface is produced by the highest frequency signals that penetrate to the base of the maximum thickness of the post-impoundment fill. Depending on texture, the 48 kHz signal penetrates from 2 to 3 m of high water content fill, whereas the 24 kHz signal can penetrate from 3 to 4 m of fill. Both 48 and 24 kHz signals attenuate rapidly in pre-impoundment materials, which are generally more varied texturally and lower in water content. Hence, the base of acoustic returns at these frequencies closely coincides with the base of post-impoundment fill. During post-survey analysis, the base of fill was traced primarily on the 48 kHz data. The 24 kHz data were used trace the base of fill in the deepest channels. Lower frequency signals would be used for reservoirs with greater maximum sediment accumulation than the 2 to 3 m maximum thickness found in Grenada Lake.

For the present survey, the sound source was suspended over the side of a Johnboat, holding the transducers at a constant dept below the surface and in a fixed position relative to the GPS antenna (Figure 2-7). Control over the transducer location is required to achieve precision water depth information and sub-meter horizontal positioning accuracy. Because the survey took about ten days to complete, all survey data were corrected by the daily records of the reservoir water elevation.

Figure 2-5. Photograph of acoustic profiler control module. All acoustic profiling and DGPS navigation electronics are contained in a compact, water-resistant control module.

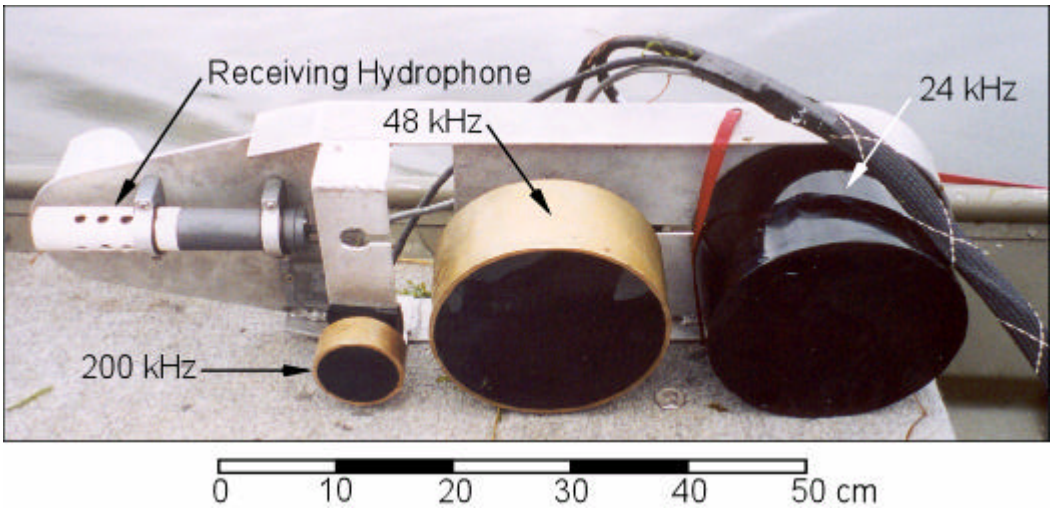

Figure 2-6. Picture of acoustic profiler transducer array. The profiling system produces acoustic signals with three widely separated frequencies (200, 48, and 24 kHz) in rapid succession as the profiles are traversed.

Figure 2-7. Picture of acoustic profiler transducer array mounted to the side of a Johnboat.

2.3 Survey Procedure

Conventional sediment surveys are conducted by collecting data along a series of parallel profiles at a set spacing that provides adequate spatial coverage, plus a number of tie lines to ensure consistency in interpretation between profiles. During the surveys, the pre-planned lines and the current boat location are displayed on the system monitor as the boat is navigated. DGPS corrections are received from U.S. Coast Guard beacons so that the location of the boat can be determined with sufficient accuracy to guide it down the line in real-time. For both surveys presented herein, strong correction signals were available from a station in Memphis.

The present survey was conducted during May, 2002 by Paul Higley and his personnel, with the assistance of the USDA-ARS National Sedimentation Laboratory.

2.4 Digital Processing and Interpretation of Collected Acoustic Data

The main difference between conventional bathymetric surveying and subsurface profiling is that subsurface profiling involves more extensive digital processing and interpretation of the collected data. During post-survey interpretation, recordings of the frequencies are combined to produce a single, false-color cross-section through the water column and sediment. In the present application, the red component of the RGB display was set to the intensity of the 200 kHz signal, the green component was set to the intensity of the 48 kHz signal, and the blue component was set to the intensity of the 24 kHz signal.

The task of the user is to identify the water bottom and the base of post-impoundment sediment and to trace these surfaces along each profile. This is again accomplished using the program *Depthpic*. The user traces the water bottom and sub-bottom surfaces by drawing on the displayed acoustic data using the computer mouse. The depth and horizontal position of each interpreted point is exported to a file that can be read by commercial mapping programs.

The base of post-impoundment sediment was identified by Bennett and Rhoton (2003) using stratigraphic and isotopic analyses of the sediment cores. This interpreted base of sediment identified in select cores was extended here and traced continuously in the reservoir and up each tributary arm. For the Grenada Lake survey a velocity of 1481 m/s was used for the average velocity of sound in water in the conversion from sound travel time to water depth. This corresponds to the speed of sound in fresh water at the local mean annual surface temperature of 67º F. Sediment thicknesses were calculated using a velocity of 1441 m/s for sediment fill. This corresponds to the speed of sound in near-bottom sediments with a composition of silty-clay.

To generate water depth maps, the interpreted depths and horizontal positions for each profile were exported from *Depthpic* to an ASCII file of x, y, z values. These data were combined with points defining the shorelines of the lake available from MARIS. The combined data were read by *Surfer*™, grided using the Kriging procedure, and contoured. The contour map generated by *Surfer*™ was exported to a drafting program to make the final figure presented herein. Volumes were computed by trapezoidal rule applied to the interval grids.

3. CORE SAMPLE LOCATIONS

Figure 3-1 shows the location of Grenada Lake in relation to local communities. The purpose of site location for the sampling program was to collect as many as 50 sediment cores along the length of the Yalobusha River arm, the Skuna River arm, and within the main pool of Grenada Lake. A hand-held GPS receiver was used to define the geospatial coordinates for all sample locations.

Figure 3-2 shows all sample locations and Table 3-1 provides the exact UTM coordinates for each site. Core locations within the lake are numbered consecutively 1 through 47, with multiple cores extracted at same location, and numbered in accordance to the date obtained. For the physical and chemical analysis of these cores, the reader is referred to Bennett and Rhoton (2003).

Table 3-1. Summary of Grenada Lake sediment cores, their date collected, and their UTM coordinates.

Core ID	Date Collected	Coordinates (UTM): NAD 83/False Easting =500000 m	
		Easting (m)	Northing (m)
1	10/17/2001	254854.1766	3755251.6268
2		253412.3511	3755634.0631
3		253409.5730	3755293.0174
4		253383.2670	3754738.2122
5		251202.8926	3754828.8772
6		250969.8545	3754673.0566
7		250473.5225	3754499.6743
8		250623.7632	3752928.0327
9	10/18/2001	249800.1444	3752602.5609
10		250081.0068	3752506.7401
11		250489.1701	3752357.6591
12		249707.3075	3750552.8643
13		249085.6820	3750731.5022
14		248530.0371	3750778.8219
15	11/16/2001	244653.2907	3744378.9397
16		244653.2907	3744378.9397
17	12/4/2001	244544.2871	3745263.3722
18		244479.0483	3746538.0785
19		246348.0526	3747752.9410
20		246184.6711	3747174.3123
21		246397.1772	3746303.5219
22	12/5/2001	246668.6157	3745703.1537
23		246891.8964	3744749.0919
24		250977.2553	3746451.0801
25		250908.5274	3745806.0558
26		251301.0535	3744853.6513
27	5/19/2002	260221.0092	3745314.2494
28	6/8/2002	260256.3438	3744681.4791
29		260173.9013	3745011.5593
30	6/9/2002	258360.3926	3745139.4440
31		258355.9805	3744795.1433
32		258358.6159	3744319.8133
33	6/16/2002	256087.5272	3744435.2546
34		256097.1202	3744796.0482
35		256057.1555	3745221.3121
36		254460.8458	3745563.9993
37		254527.9720	3744783.9983
38		254453.4148	3744367.4512
39		250803.8211	3744572.7729
40		250131.9704	3744083.8097
41		249181.7191	3743864.7320

Table 3-1 continued.

Core ID	Date Collected	Coordinates (UTM): NAD 83/False Easting =500000 m	
		Easting (m)	Northing (m)
42	6/19/2002	249332.5348	3747342.4269
43	6/19/2002	249007.5953	3746379.2637
44	6/20/2002	246910.5677	3744741.4264
45	10/1/2002	251950.8213	3754221.4620
46		249701.7919	3750541.4605
47		250494.2464	3752368.7526

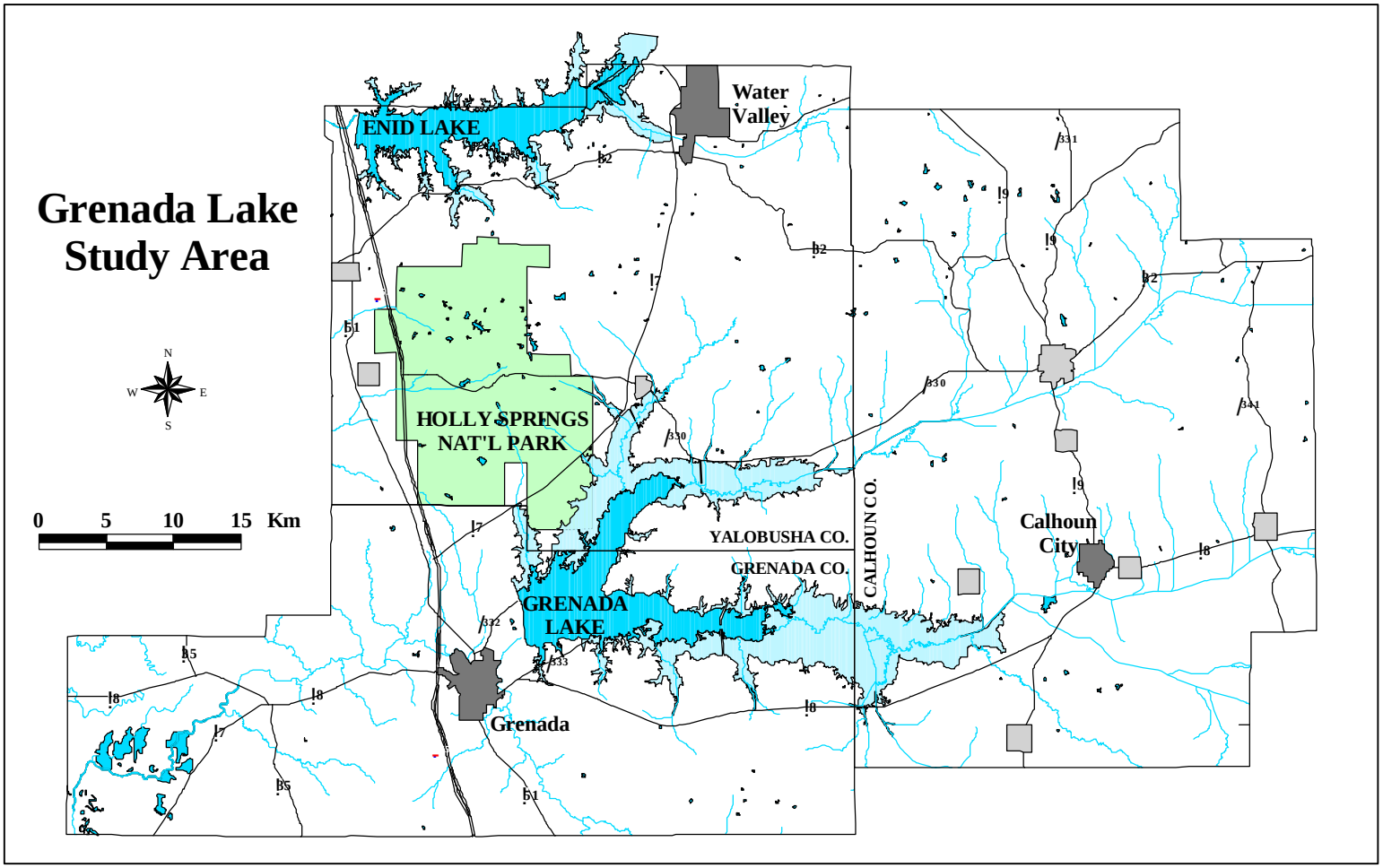

Figure 3-1. Map showing Grenada Lake and surrounding environs.

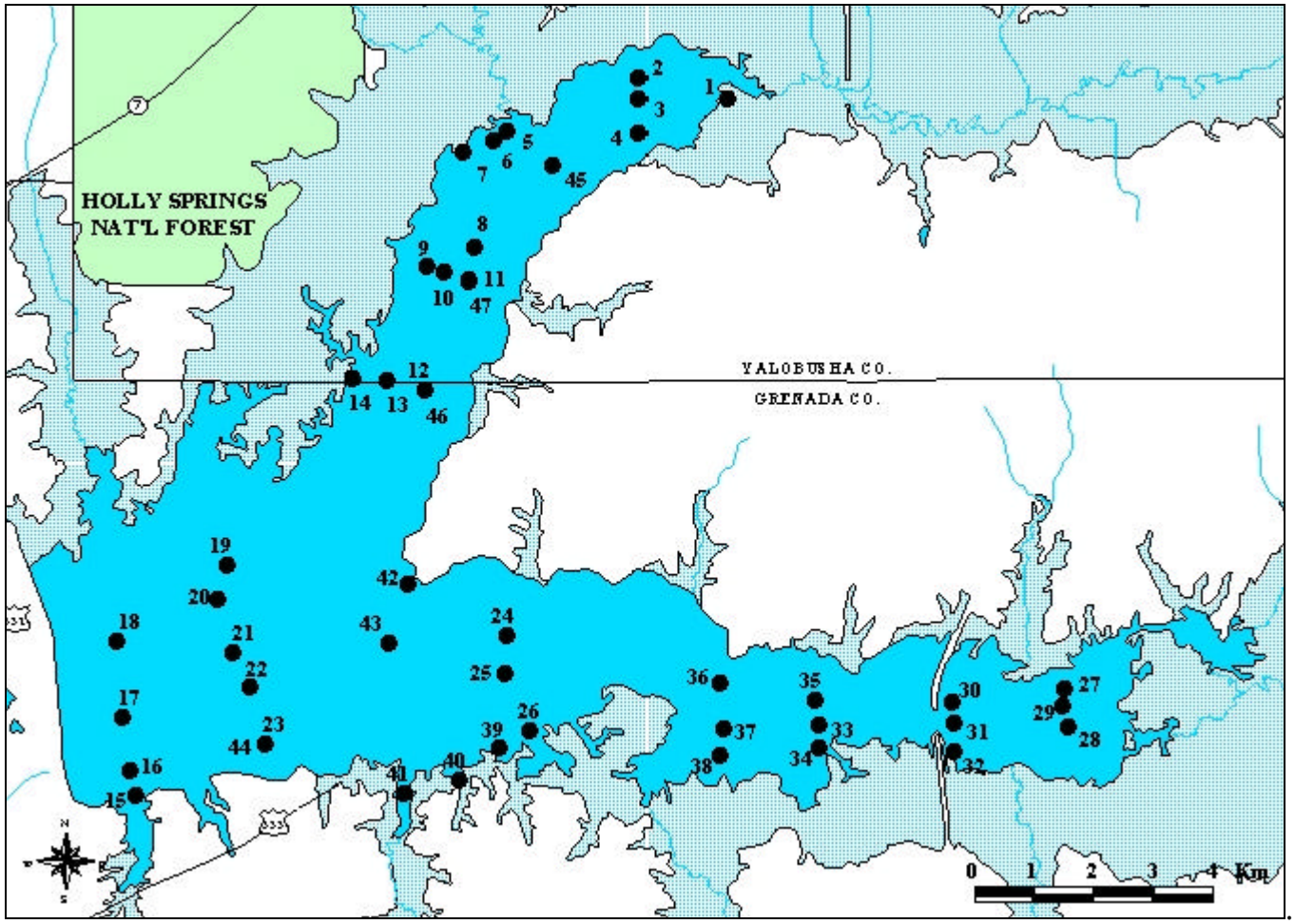

Figure 3-2. Map showing the locations of all cores in Grenada Lake study area.

4. RESULTS

Bennett and Rhoton (2003) presented the core data from Grenada Lake and their stratigraphic interpretation. Because the interpretation of the geophysical data relies so heavily upon the stratigraphic information, this discussion is repeated here. This interpretation is then extended to the geophysical data collected.

4.1 Discriminating Between Pre- and Post-impoundment Sediment Deposition

As discussed in Bennett and Rhoton (2003), the presentation and interpretation of the physical and chemical characteristics of the sediment within Grenada Lake depends on discriminating the post-impoundment sediment, or sediment that has accumulated since the construction of the dam, from the pre-impoundment sediment, or sediment that was present prior to the construction of the dam. This interpretation is based on the following evidence: (1) the use of chemical isotopes and their geochronological interpretation, and (2) variations in sediment texture and bulk density with depth. Two cores were chosen for this analysis: Core 22 and Core 43.

4.1.1 Use of Isotopes for Geochronological Interpretation

Two sediment cores were analyzed for radioactive lead (^{210}Pb; 22-year half-life) for the purpose of dating sediment horizons. Lead-210 is a natural product of the decay of ^{222}Rn gas, the daughter of ^{226}Ra, in the atmosphere (Binford and Brenner, 1986). The flux of ^{210}Pb to sediments in most lakes is across the air-water interface, with negligible supply from tributaries or terrestrial sources. Small quantities of ^{210}Pb are produced within lake sediments by the decay of ^{226}Ra. This fraction is called "supported" ^{210}Pb. "Unsupported" ^{210}Pb is that fraction delivered to the sediments from atmospheric fallout. The amount of unsupported ^{210}Pb in a sediment sample can be calculated by measuring both the ^{210}Pb and ^{226}Ra concentrations and subtracting the supported or in situ component. From this, a rate of accumulation can be derived.

Two sediment cores were analyzed for radioactive cesium (^{137}Cs; 30-year half-life) for the purpose of dating sediment horizons. Because ^{137}Cs is produced during nuclear fission, its presence in the environment is due to nuclear testing or releases from nuclear reactors (Ritchie and McHenry, 1990). First global deposition of ^{137}Cs occurred in 1954±2 and maximum deposition occurred in 1964±2 in the Northern Hemisphere, related to above ground nuclear testing, and in 1986 (Europe) due to the Chernobyl nuclear accident. Cesium-137 concentration can be used as a unique tracer for erosion and sedimentation because it is strongly adsorbed to clay and organic particles and is essentially non-exchangeable. The following assumptions are made herein: (1) ^{137}Cs falls onto the lake surface and attaches quickly to the suspended sediment in the water column, and (2) sediment deposition occurs shortly thereafter. However, surface soil particles eroded from the landscape may be another source of ^{137}Cs. Rates of sediment accumulation can be calculated by knowing the depth of these different ^{137}Cs horizons.

Sediment samples for ^{210}Pb and ^{137}Cs analyses were sent to Flett Research Ltd., Winnipeg, Canada. For ^{137}Cs analysis, dried and ground sediment is compressed at 10,000 PSI into a 2-1/8 inch diameter pancake and placed into an aluminum foil planchet. The sample is placed onto an

Ortec GEM High Purity Germanium Coaxial detector (efficiency 18%) and completely surrounded by 2 inch lead shielding. The emission of ^{137}Cs is quantified by comparing the sample's counts per second with a NIST spiked clay gamma-ray emission-rate standard. The detection limit for a period of 80000 seconds is on the order of 0.5 DPM/g (detections per minute per gram) for a 10-g sample. The ^{210}Pb analysis is based on quantifying the amount of polonium-210 (^{210}Po; a grand-daughter of the ^{210}Pb decay sequence) in the sediment sample. The polonium is converted to chloride and distilled from the sediment at 500°C. The ^{210}Po distillate is digested in nitric acid, converted to a chloride salt, and precipitated onto a silver disk. The silver disk is placed into an Ortec alpha spectrometer for an 8-hour counting period and monitored for ^{210}Po and ^{209}Po isotopes as compared to the activity of a ^{209}Po spike added at the beginning of sample processing. Detection limits are on the order of 0.1 DPM/g (0.0017 Bq/g) for an 8-hour counting period using a 0.5-g sample.

4.1.2 Geochronological Results and Interpretations for Core 22

Figure 4-1 shows the geochronological results obtained for Core 22, plotted alongside the variation of sediment texture and sediment bulk density with depth. There is an exponential drop in the ^{210}Pb activity as a function of depth from 0 to 0.4 m. The surface activity is about 5 times the estimated average background ^{210}Pb (1.6 DPM/g) of the lower 0.5 m of the core. The sediment core shows two different sedimentation rates. Cesium-137 is approximately evenly distributed through the upper 0.3 m of the core (0.6 DPM/g), increases to 1.2 DPM/g in the 0.3 to 0.4 m section, and peaks at 2.3 DPM/g in the 0.4 to 0.5 m section.

The slope regression model of unsupported ^{210}Pb activity versus cumulative dry weight (g/cm^2) includes the upper 0.4 m of the core. The slope model assumes constant sedimentation and ^{210}Pb input. If the average ^{210}Pb activity of the deepest sections of the core (1.6 DPM/g) is the true background, then the closest corresponding sediment accumulation rate is about 0.4053 g/cm^2-yr, and this is has an associated background level of 1.5161 DPM/g. The regression plot, using 1.5161 DPM/g as background, is shown in Figure 4-1a.

Using a sedimentation rate of 0.4053 g/cm^2-yr, the age of the sediment at a depth of 0.4 m is calculated as cumulative mass (12.83 g/cm^2) divided by the sedimentation rate (0.4053 g/cm^2-yr), which is 31.66 years. The core was sampled in 2002, the date at 0.4 m depth would be about 1970 (Figure 4-1a). Using a dam construction date of 1954 and assuming a sedimentation rate of 0.4053 g/cm^2-yr), the calculated cumulative mass for this time period would be 19.45 g/cm^2, which corresponds to a depth of 0.5 m (Figure 4-1a).

For Core 22, the peak ^{137}Cs activity occurs at a depth of 0.4 to 0.5 m and little to no activity occurs below this level. It is concluded that this peak corresponds to the 1964 timeline, and the reduced activity at a depth of 0.5 to 0.6 m corresponds to the date of dam construction (1954; Figure 4-1c). These timelines derived correlate well the timelines determined using the ^{210}Pb data.

These timelines also correspond to depth variations in sediment texture and bulk density. Assuming that dam construction correlates to a subsurface depth of 0.5 m, the post-impoundment sediments are enriched in clay (up to 80% by mass) and depleted in both silt (about 20% by

mass) and sand (about 0% by mass) as compared to the parent or pre-impoundment materials, which has more silt (up to 60% by mass) and sand (up to 5% by mass) and less clay (up to 35% by mass; Figure 4-1d). Moreover, the pre-impoundment sediments are denser (greater than 1400 kg/m^3) than the post-impoundment sediments (less than 1100 kg/m^3; Figure 4-1e), although this may be the results of compaction and dewatering due to burial.

4.1.3 Geochronological Results and Interpretations for Core 43

Figure 4-2 shows the geochronological results obtained for Core 43, plotted alongside the variation of sediment texture and sediment bulk density with depth. There is an irregular drop in the ^{210}Pb activity as a function of depth in the upper 0.8 m (or 80 g/cm^2) of core (Figure 4-2a). The surface activity is about two times the estimated average background ^{210}Pb activity level (1.076 DPM/g) of the deepest six sections. The ^{210}Pb activity data indicate varying sedimentation rates for this core.

The ^{137}Cs activity is undetectable in the upper portions of the core (0 to 0.1 m) and low for the middle portions (0.1 to 0.2 pCi/g for 0.1 to 0.5 m; Figure 4-2b). The peak in ^{137}Cs activity (about 0.6 pCi/g) occurs at a depth of 0.7 to 0.8 m. This peak is interpreted as the 1964 timeline. The significant ^{137}Cs activity observed above and below the maximum is attributed to post-depositional diffusion of the isotope or mixing within the sediments. The relatively constant ^{210}Pb activity observed in the deepest sections of the core is assumed to represent background levels.

Based on this information, sediment located at a depth of 0.9 m would have been deposited prior to 1958, or near the time the dam was constructed (1954). If the initial surface activity of ^{210}Pb in the core is assumed to be about 2 DPM/g, and the background is 1 DPM/g, then the surface excess ^{210}Pb would be only about 1 DPM/g. After nearly 44 years (or two half-lives of ^{210}Pb), the excess activity would drop to about 0.25 DPM/g, and this would not be significantly different from background. Thus, the observed ^{210}Pb profile in Core 43 is not at odds with the ^{137}Cs activity results. However, the slope regression model for ^{210}Pb cannot be applied here because a constant rate of sedimentation, i.e., a monotonic decrease in ^{210}Pb activity, is not observed.

In addition, the dam construction timeline derived from ^{137}Cs activity data does not correlate well with the variation in texture and bulk density (Figure 4-2c and d). There is a slight trend for clay to be enriched from a depth from 0.9 to 0.55 m within the core. Also, sediment bulk density is higher below the 1954 timeline (Figure 4-2b).

4.1.4 Discussion

Figures 4-1 and 4-2 show that the ^{137}Cs activity data within the sediments can be used to define the stratigraphic position of dam construction. Results from Core 22 show that the timelines derived from the ^{210}Pb data correlate well with the ^{137}Cs data. Moreover, these timelines also correspond to depth variations in sediment texture and bulk density. That is, the post-impoundment sediments are enriched in clay (up to 80% by mass) and depleted in both silt (about 20% by mass) and sand (about 0% by mass) as compared to the parent or pre-impoundment materials. The lack of correlation between the ^{137}Cs data and sediment texture in

Core 43 may be due to (1) the mixing of sediment sources or (2) the dispersal or movement of sediment after deposition as the result of dam operation.

Based on the results obtained for Core 22, the interpretation of the physical and chemical characteristics of the sediment will be based on whether the materials have accumulated since dam construction. These interpretations will be based on the variations in sediment texture, which show the significant enrichment in clay content since construction. Those sediment cores that show ambiguous textural trends will not be interpreted in this manner.

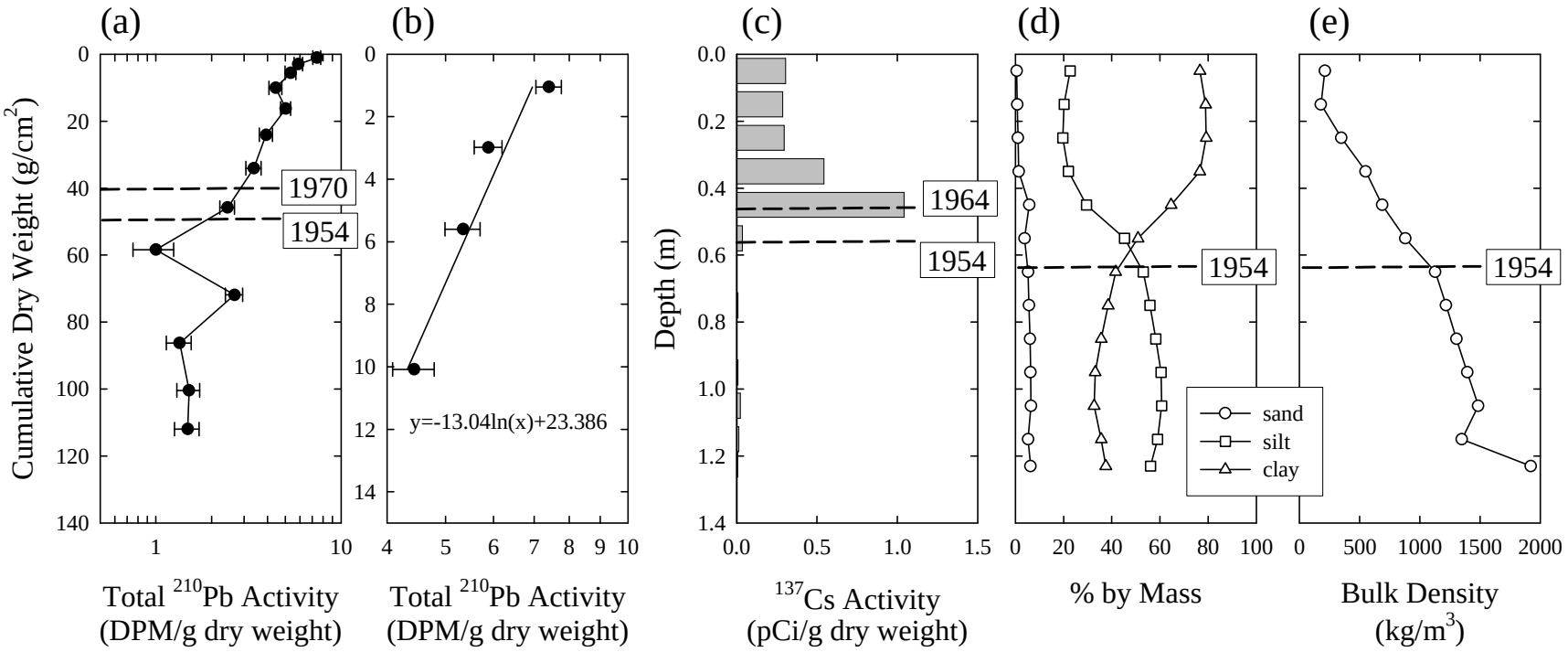

Figure 4-1. Geochronological results and interpretations for Core 22 showing (a) ^{210}Pb activity as a function of cumulative dry weight of sediment, (b) regression model for ^{210}Pb activity for the upper portion of the core, (c) ^{137}Cs activity as a function of core depth, variation of (d) sediment texture and (e) sediment bulk density with core depth. Interpreted timelines (1954, 1964, and 1970) are also shown. See Figure 3-2 for core location.

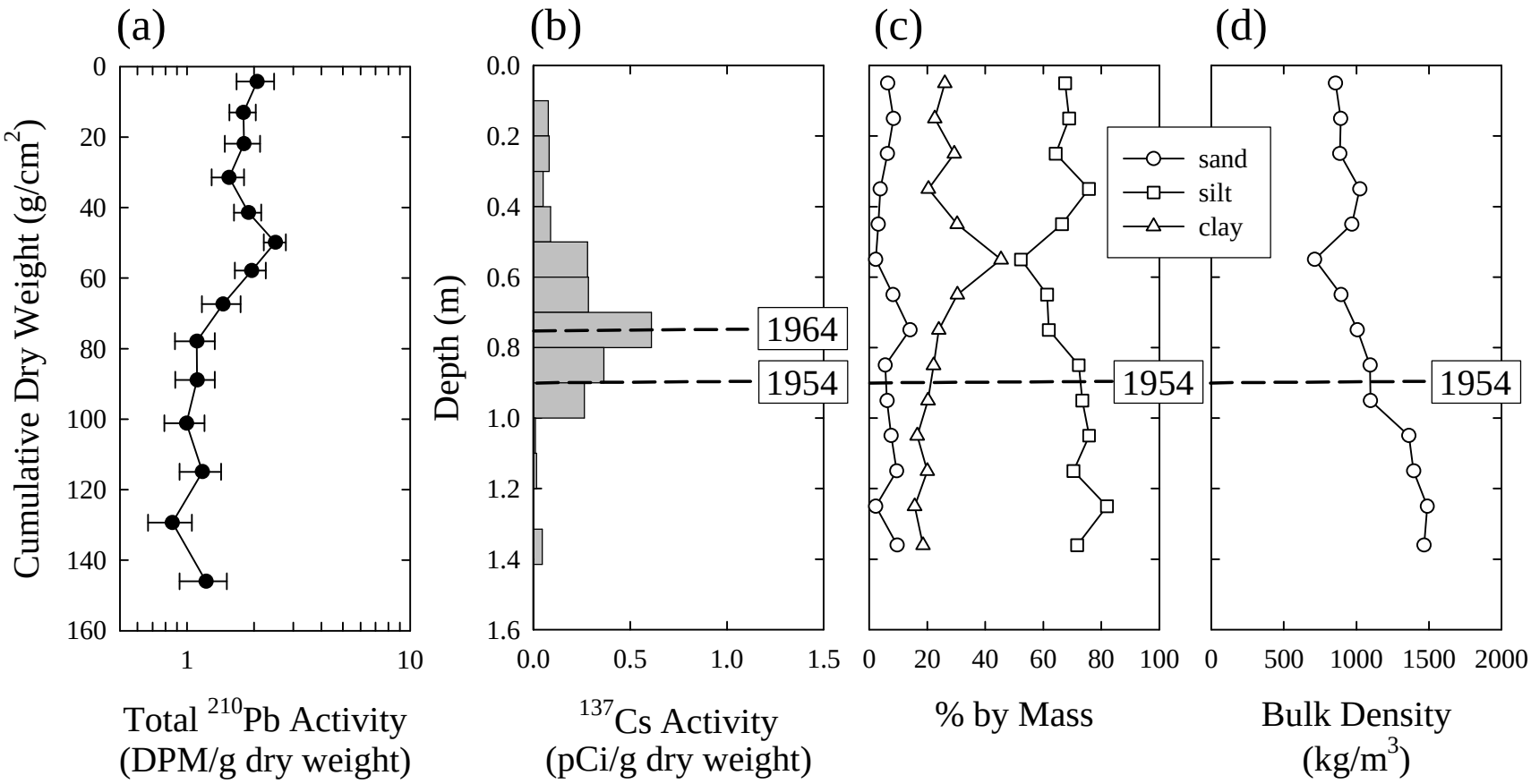

Figure 4-2. Geochronological results and interpretations for Core 43 showing (a) ^{210}Pb activity as a function of cumulative dry weight of sediment, (b) ^{137}Cs activity as a function of core depth, variation of (c) sediment texture and (d) sediment bulk density with core depth. Interpreted timelines (1954 and 1964) are also shown. See Figure 3-2 for core location.

4.2 Application of Geochronology to Cores with Particle Size Data

The geochronological data presented above provides the necessary criterion for determining the division between post-impoundment sedimentation and pre-impoundment or parent material. This criterion is the significant enrichment of clay-sized particles and the depletion of silt-sized particles, and it has been applied to all sediment cores where textural variations are unambiguous (Figures 4-3 and 4-4). Table 4-1 lists the depth to the 1954 horizon—the time of dam construction—for all cores successfully interpreted. The greatest sedimentation occurs in the upper reaches of the Yalobusha River, where as much as 1.2 to 1.3 m of sediment has accumulated since dam construction (Table 4-1; Figure 4-4). Within the main pool of Grenada Lake, the enrichment of clay-sized particles and the depletion of silt-sized particles are most apparent, and sediment accumulations are typically 0.5 to 0.9 m.

Table 4-1. Depth to 1954 horizon (time of dam construction) for those cores with particle size data and based on geochronological interpretation. Not all cores with particle size data were interpreted in this manner. Refer to Figures 4-3 and 4-4.

Core Number	Depth to 1954 horizon (m)
1	0.8
8	0.4
12	0.7
16	0.9
21	0.5
22	0.7
24	0.5
27	0.8
31	1.3
34	0.8
36	1.2
43	0.7
44	0.7

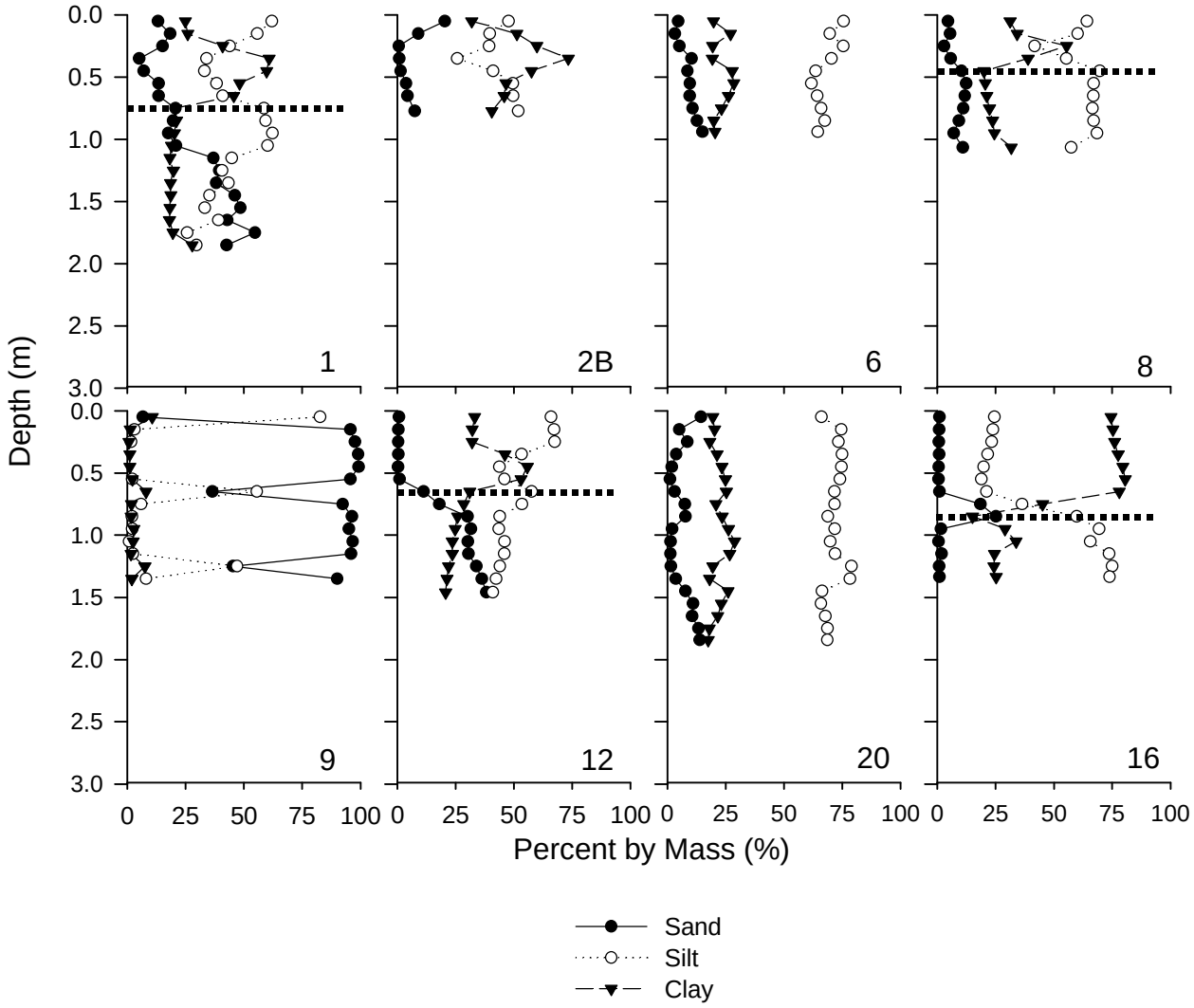

Figure 4-3. Variations in sediment texture with depth for select cores along the Skuna River arm of Grenada Lake, starting upstream (Core 1) and traversing into the main pool (Core 16). The dashed line demarcates the division between post-impoundment deposition and pre-impoundment sediment materials that could be interpreted with the geochronological data. Refer to Figure 3-2 for core locations.

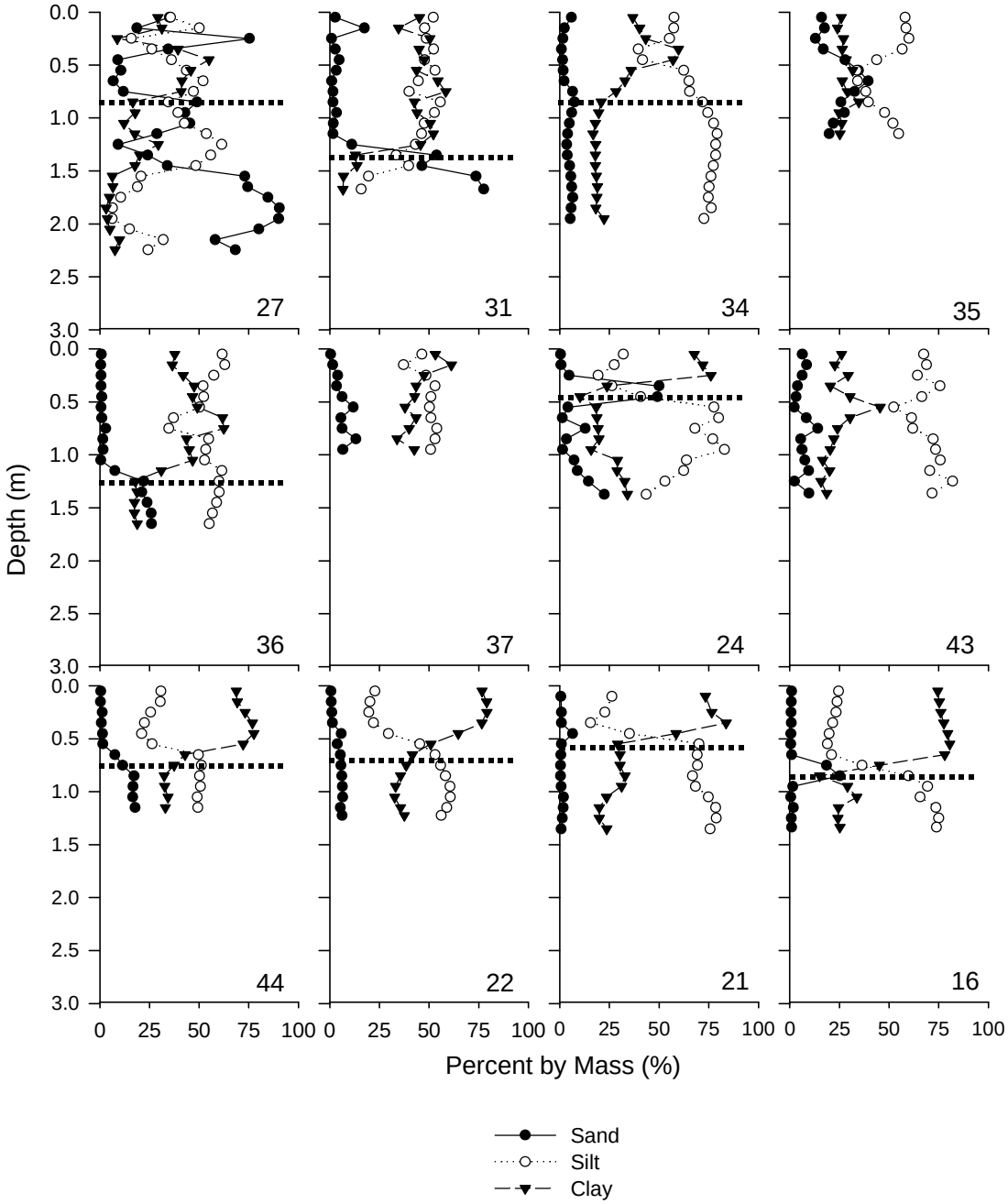

Figure 4-4. Variations in sediment texture with depth for select cores along the Yalobusha River arm of Grenada Lake, starting upstream (Core 27) and traversing into the main pool (Core 16). The dashed line demarcates the division between post-impoundment deposition and pre-impoundment sediment materials that could be interpreted with the geochronological data. Refer to Figure 3-2 for core locations.

4.3 Acoustic Survey

Figure 4-5 shows the geophysical survey lines for Grenada Lake. A total of 440 linear km (273 linear miles) of data were collected as part of this study. Also shown on this map are core locations used to interpret the seismographs and survey line numbers used in the examples below.

Using the results of the stratigraphic analysis presented above, Figures 4-6 to 4-12 plot processed acoustic data, the relative (projected) position and thickness of the post-impoundment sediment core used to interpret the data (Figures 4-3 and 4-4), and the horizons that signify the top of the sediment (in red) and the depth to the as-built or pre-impoundment surface (in yellow). The width of this horizon represents the thickness of the deposited sediment at-a-point since dam construction.

In general, there is very good agreement between the acoustically-determined horizons and the stratigraphically-determined post-impoundment sediment thickness. The difference between these two surfaces, see for example Figures 4-8 and 4-10, is due to projecting the core results, which can be as much as 160 m away, onto the seismograph. As shown below, sediment thickness within the lake can vary marked over short distances.

The pattern of sedimentation depends on the pre-existing lake bathymetry. In Figure 4-13, two processed seismographs are shown, delineating the pre-impoundment sediment surface in yellow. Sediment tends to be thicker in the topographic lows, or in this case the relict or drowned Yalobusha and Skuna River channels, as compared to the plateaus on either side representing the relict floodplains. Several examples of this variation in sediment thickness are observed in the processed acoustic data. In some cases, the difference in post-impoundment sediment thickness between these two neighboring areas can be as much as a factor of 7. This suggests that the incised, relict channels are playing some role in concentrating, moving, and storing impounded sediment as a response to sediment deposition and normal operation of the reservoir.

The distribution of accumulated sediment since dam construction is shown in Figure 4-14. Although there are small pockets of very thick sediment, >2 m, the impounded sediment in the arms of the Yalobusha and Skuna Rivers is about 0.5 to 1.0 m thick and about 1.5 m thick in the main pool of the lake. Sediment thickness tends to increase towards the pool region. This pattern of sedimentation is consistent with the stratigraphic results presented above.

It should be noted that this isopach map shows the distribution of impounded sediment in the main portion of the lake, which is composed predominately of silt and clay. This map does not include any post-impoundment sedimentation in the tributary streams. Presumably, sand deposition has occurred and is actively occurring in the tributaries well above the lake. These deposits were not surveyed and their thickness may exceed those accumulation rates reported herein.

The total volume of accumulated sediment based on these results is 40,357 ac-ft (49,790,128 m^3), assuming that sediment thickness is zero at the lake shoreline. The as-built flood control

storage is 1,251,710 ac-ft at a pool elevation of 231 ft. Using these values, the loss of flood control storage due to reservoir sedimentation since dam construction is approximately 3.3%. Thus, the reservoir has an annual storage loss of about 0.1%. These accumulation rates do not include sedimentation within the tributaries upstream of the lake and are restricted in space to those areas surveyed.

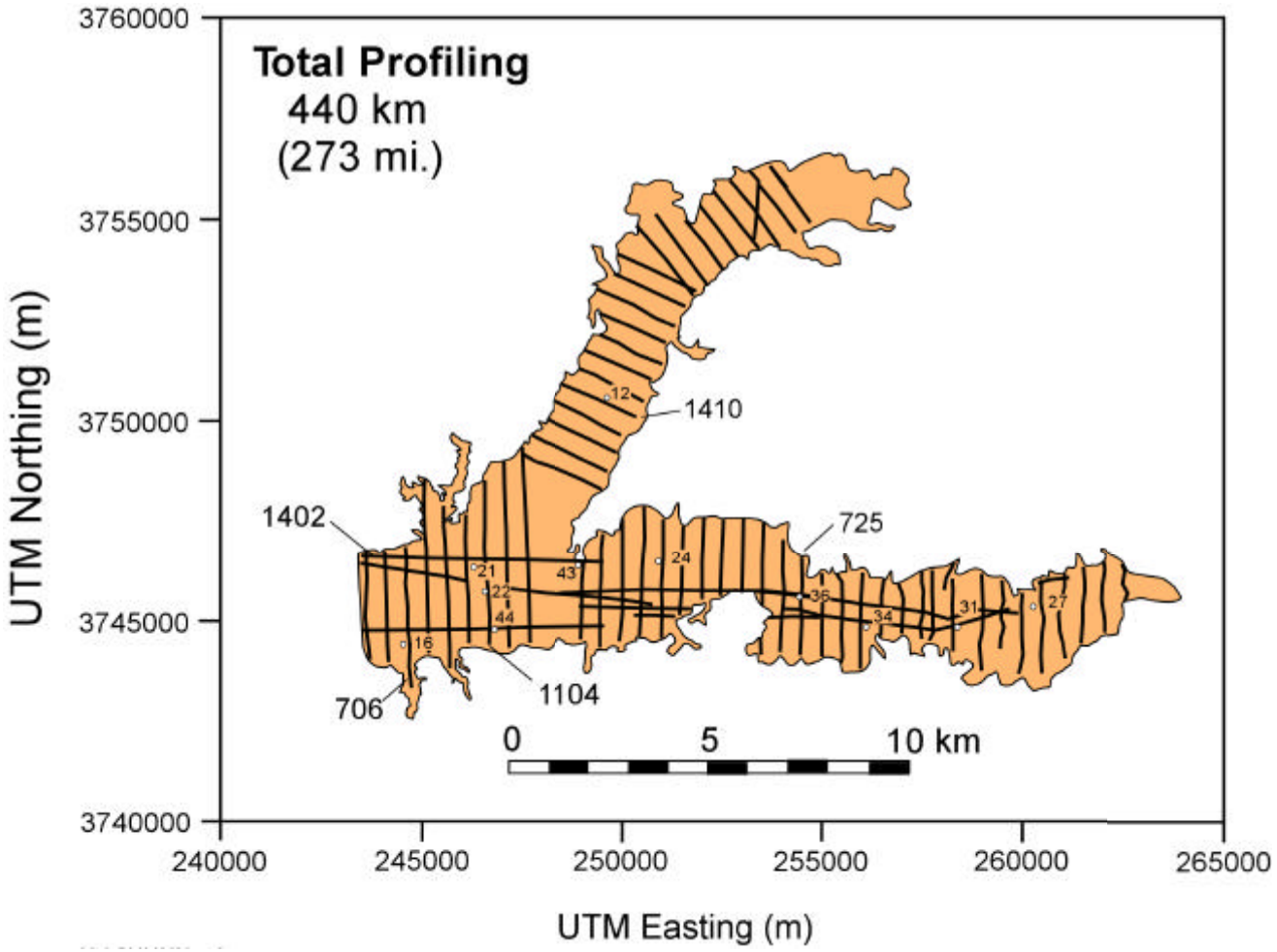

Figure 4-5. Map showing the location of all geophysical survey lines, locations of cores used for comparison, and the survey line numbers used in the examples given below. Total length of the profiles is 440 linear km (273 linear miles). Coordinates are in meters (UTM).

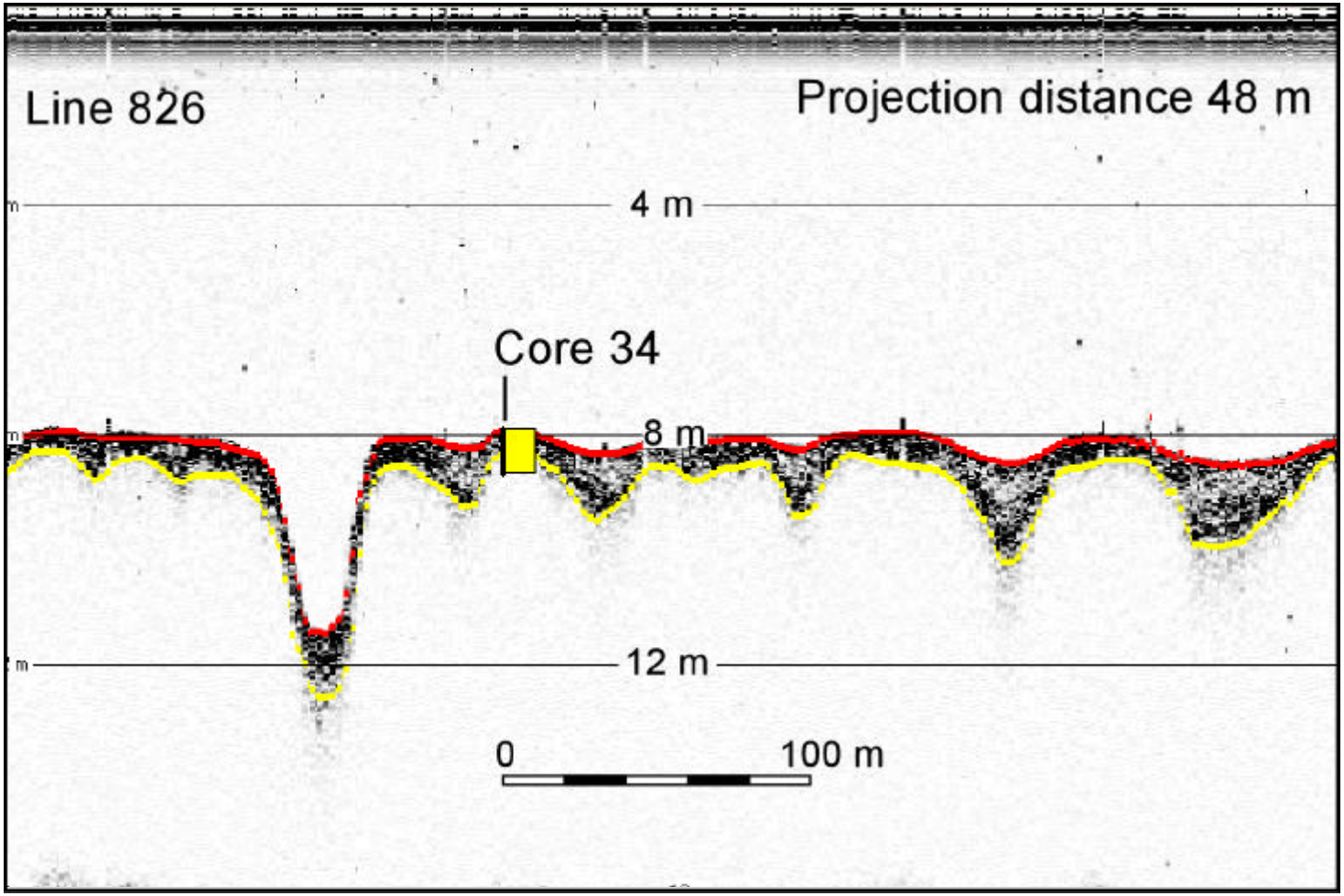

Figure 4-6. Processed and interpreted acoustic profile line showing the projection of the post-impoundment sediment Core 34 (projection distance is shown). Horizontal lines are depths below the water surface in meters, the red line is the top of the sediment surface, and the yellow line is the base of the interpreted post-impounded sediment. Horizontal scale is shown (note vertical exaggeration). See Figures 3-2 and 4-5 for core and acoustic line location.

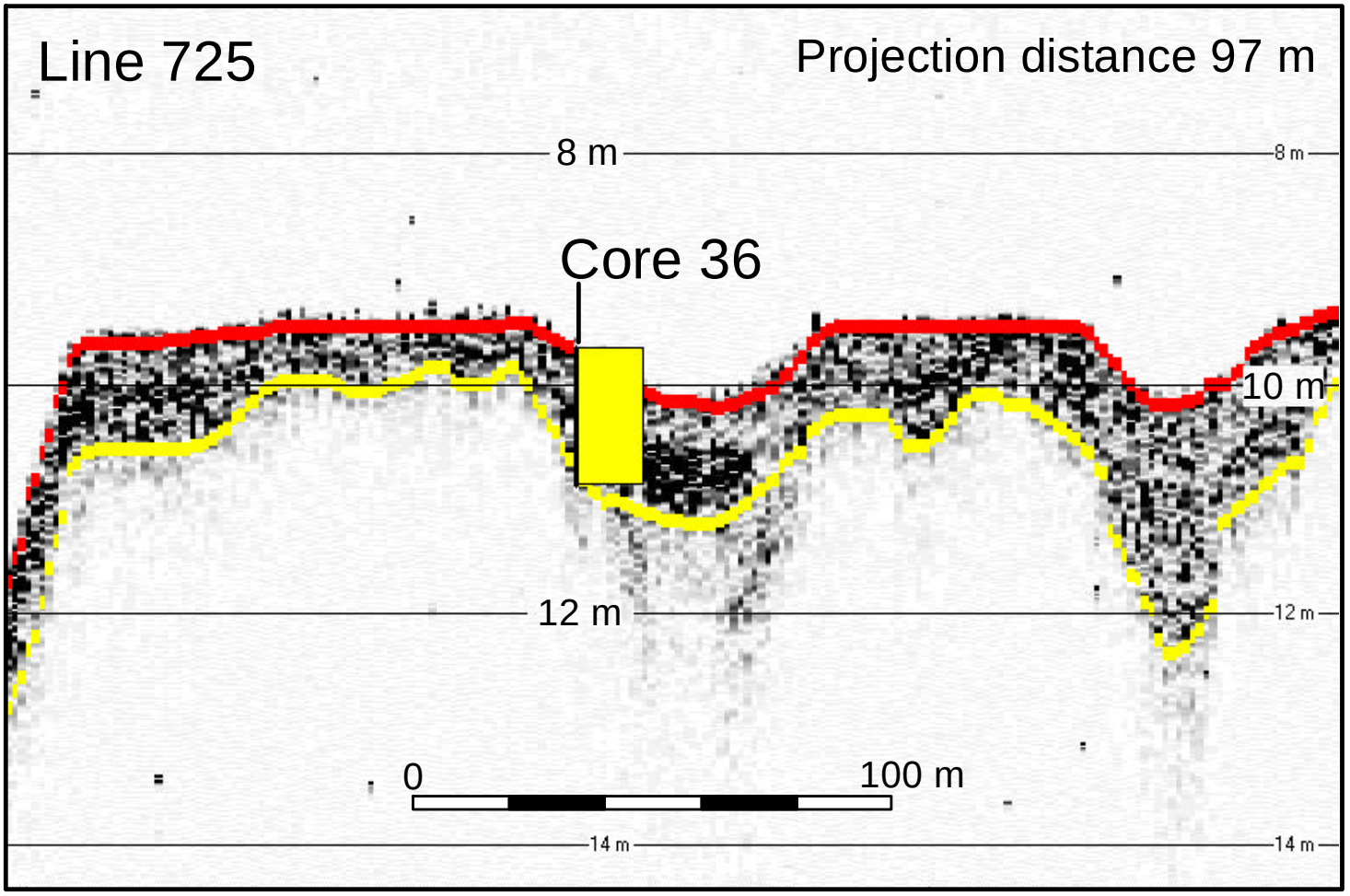

Figure 4-7. Processed and interpreted acoustic profile line showing the projection of the post-impoundment sediment Core 36 (projection distance is shown). Horizontal lines are depths below the water surface in meters, the red line is the top of the sediment surface, and the yellow line is the base of the interpreted post-impounded sediment. Horizontal scale is shown (note vertical exaggeration). See Figures 3-2 and 4-5 for core and acoustic line location.

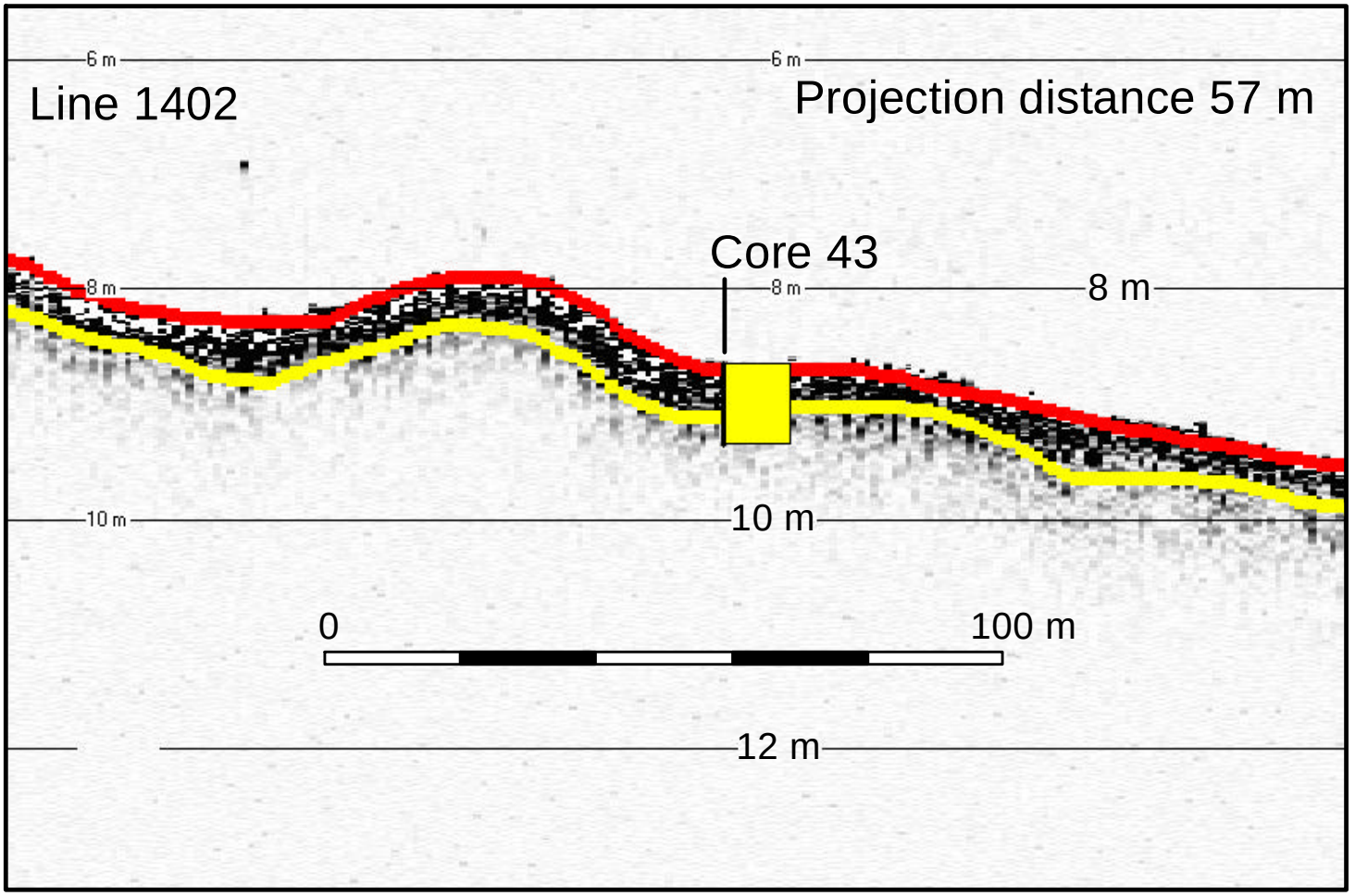

Figure 4-8. Processed and interpreted acoustic profile line showing the projection of the post-impoundment sediment Core 43 (projection distance is shown). Horizontal lines are depths below the water surface in meters, the red line is the top of the sediment surface, and the yellow line is the base of the interpreted post-impounded sediment. Horizontal scale is shown (note vertical exaggeration). See Figures 3-2 and 4-5 for core and acoustic line location.

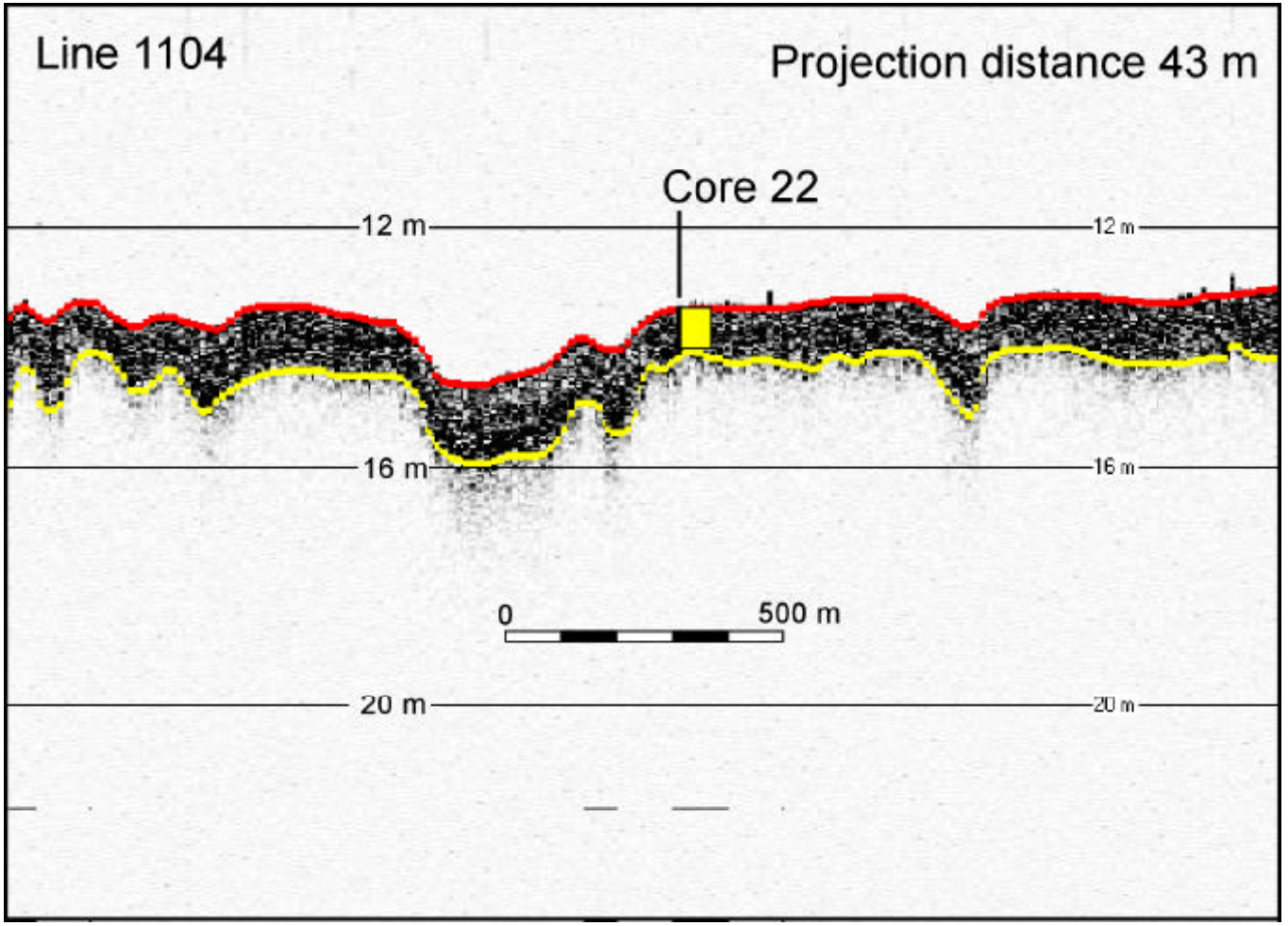

Figure 4-9. Processed and interpreted acoustic profile line showing the projection of the post-impoundment sediment Core 22 (projection distance is shown). Horizontal lines are depths below the water surface in meters, the red line is the top of the sediment surface, and the yellow line is the base of the interpreted post-impounded sediment. Horizontal scale is shown (note vertical exaggeration). See Figures 3-2 and 4-5 for core and acoustic line location.

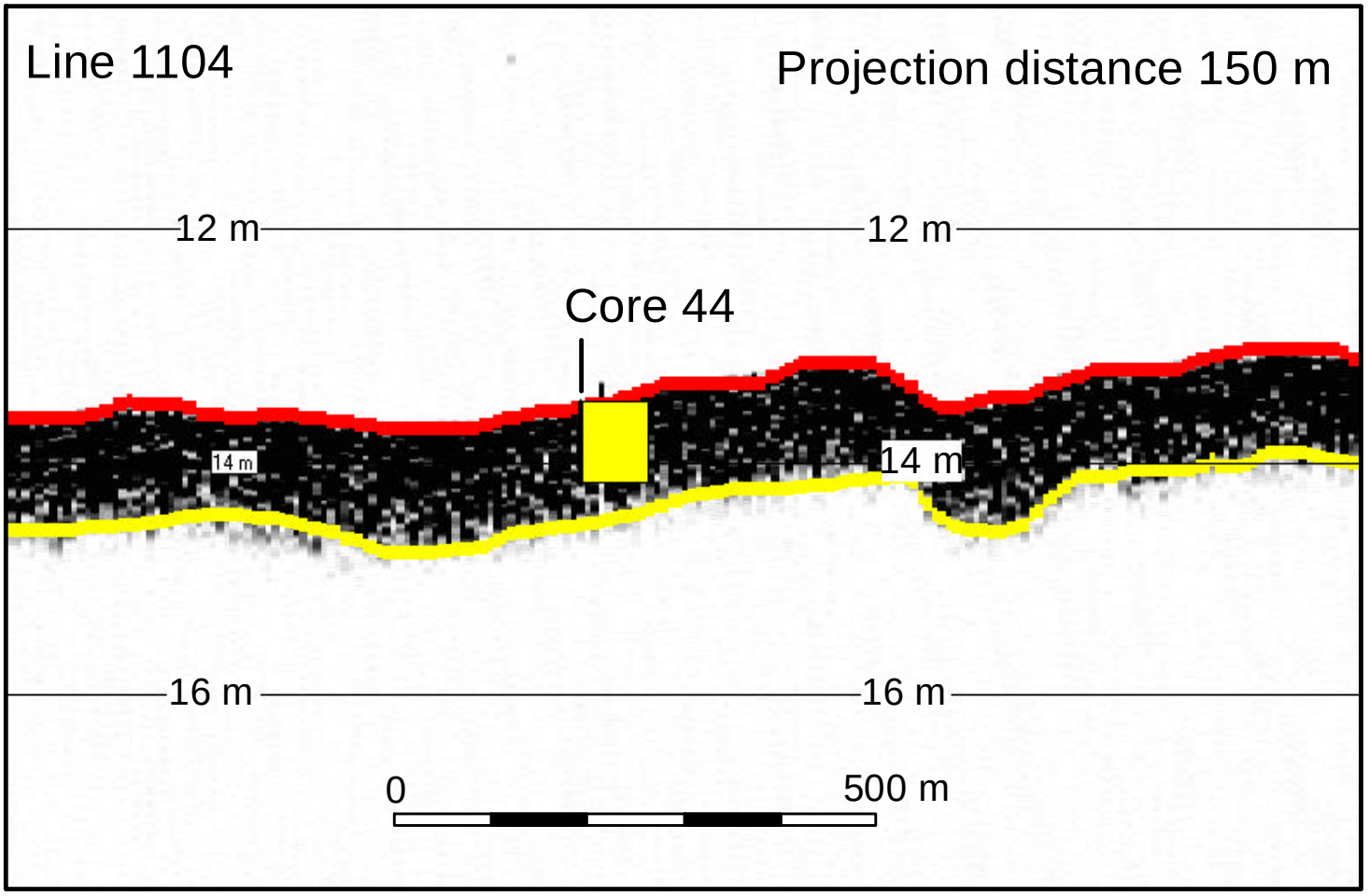

Figure 4-10. Processed and interpreted acoustic profile line showing the projection of the post-impoundment sediment Core 44 (projection distance is shown). Horizontal lines are depths below the water surface in meters, the red line is the top of the sediment surface, and the yellow line is the base of the interpreted post-impounded sediment. Horizontal scale is shown (note vertical exaggeration). See Figures 3-2 and 4-5 for core and acoustic line location.

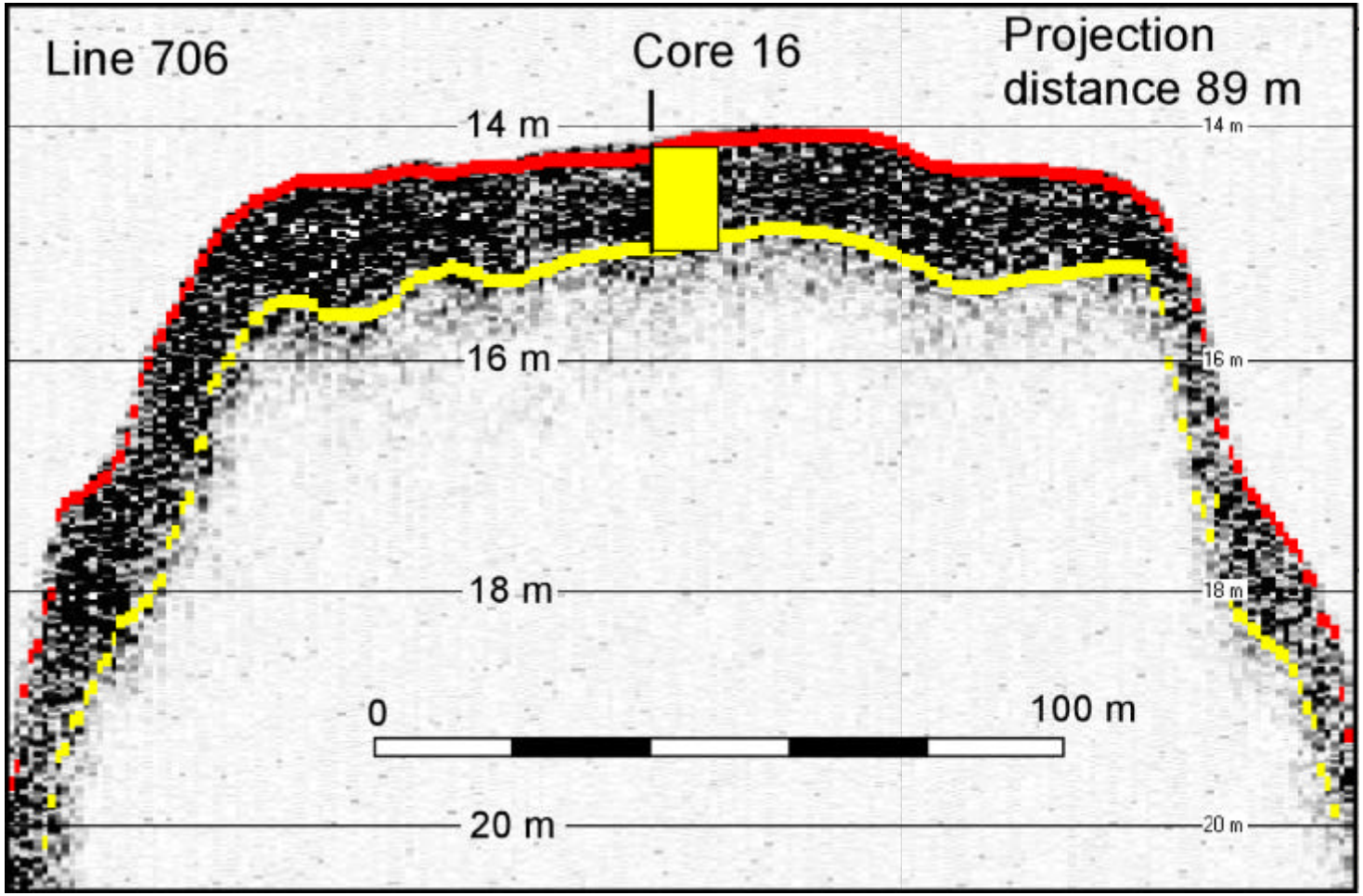

Figure 4-11. Processed and interpreted acoustic profile line showing the projection of the post-impoundment sediment Core 16 (projection distance is shown). Horizontal lines are depths below the water surface in meters, the red line is the top of the sediment surface, and the yellow line is the base of the interpreted post-impounded sediment. Horizontal scale is shown (note vertical exaggeration). See Figures 3-2 and 4-5 for core and acoustic line location.

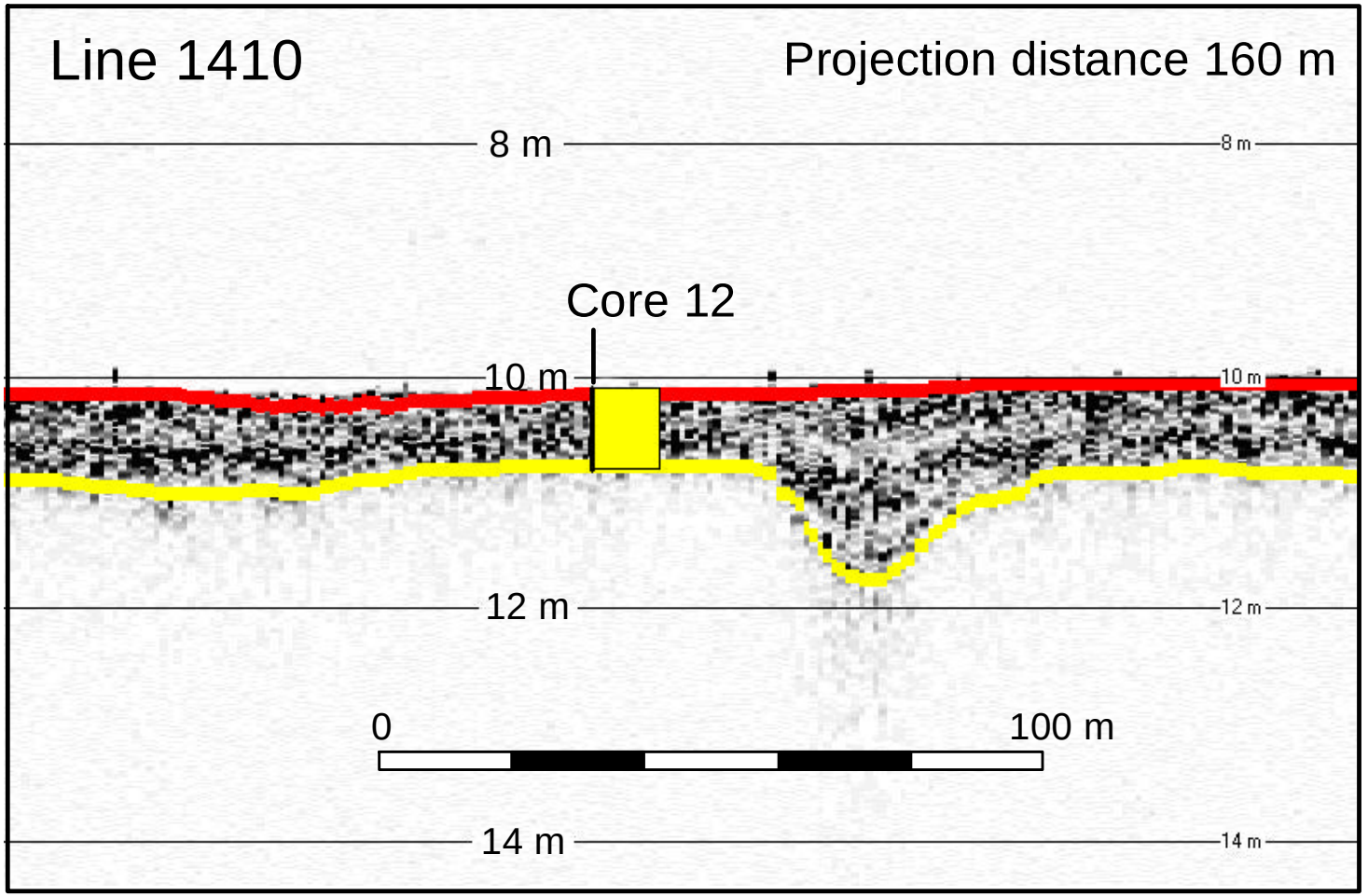

Figure 4-12. Processed and interpreted acoustic profile line showing the projection of the post-impoundment sediment Core 12 (projection distance is shown). Horizontal lines are depths below the water surface in meters, the red line is the top of the sediment surface, and the yellow line is the base of the interpreted post-impounded sediment. Horizontal scale is shown (note vertical exaggeration). See Figures 3-2 and 4-5 for core and acoustic line location.

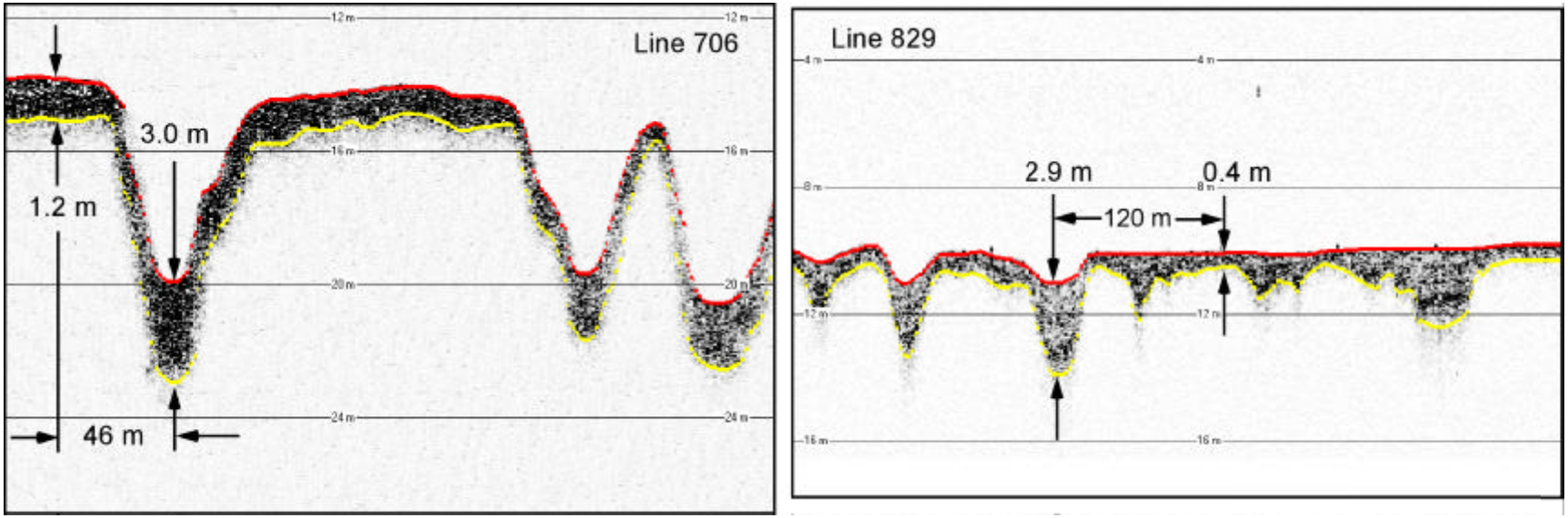

Figure 4-13. Processed and interpreted acoustic profile lines showing the variation in post-impoundment sediment thickness with distance. Horizontal lines are depths below the water surface in meters, the red line is the top of the sediment surface, and the yellow line is the base of the interpreted post-impounded sediment. Horizontal scales are shown (note vertical exaggeration). See Figure 4-5 for acoustic line locations.

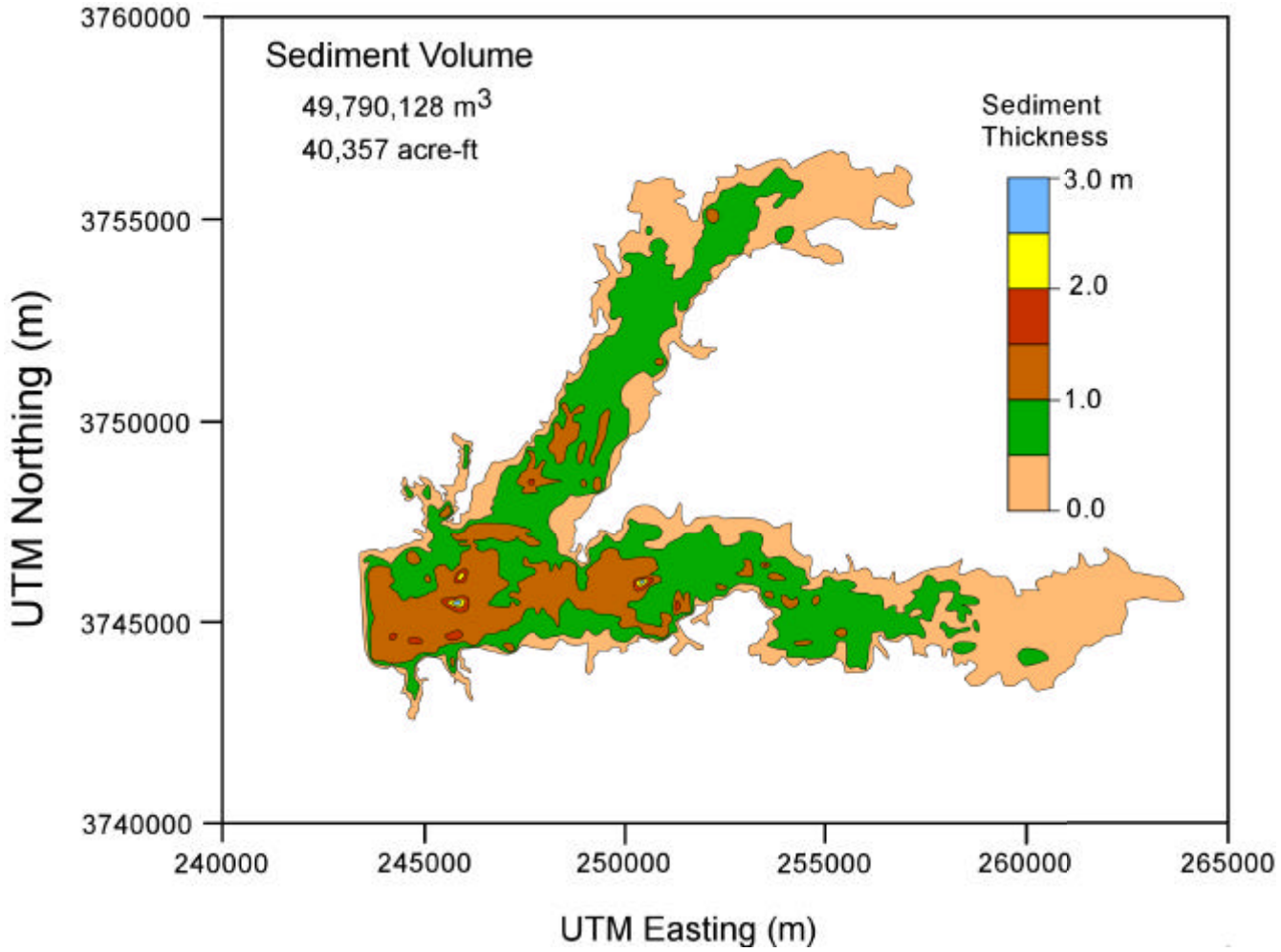

Figure 4-14. Contour map of sediment thickness in Grenada Lake. Coordinates are in meters (UTM).

5. CONCLUSIONS

Streams and rivers within the Yalobusha River basin, located in north-central Mississippi, have experienced severe erosion, bed incision, and channel widening due to channelization projects during the early 1900s and again in the 1950s and 1960s. Straightening of the Yalobusha River and Topashaw Creek has markedly altered the base level of these streams and promoted basin-wide degradation of the river channels. The primary results of this base level change were channel incision, bank destabilization, and channel widening. Large volumes of sediment and woody riparian vegetation were delivered to the flow and were transported through the river network. When the channelized, straightened Yalobusha River reaches met the natural, unchannelized meanders, the woody debris in transport was deposited. These processes, left unrequited for decades, resulted in the rapid accumulation of a large woody debris plug on the lower Yalobusha River downstream of Calhoun City. As much as 5 m of sediment and debris has accumulated vertically since 1967 and input of vegetation due to bank failure in the vicinity of major knickpoints is around 28 m^3/yr. This debris accumulation has significantly increased the magnitude, frequency, and severity of flooding within Calhoun City, MS.

Before the U.S. Army Corps of Engineers initiates debris plug removal and channel improvements, an assessment of sedimentation within Grenada Lake located downstream of the plug is required. This report summarizes research results collected to meet this need, and the main conclusions are listed below.

1. Forty-seven continuous sediment cores, ranging in length from 0.55 to 2.55 m, were collected within Grenada Lake. Select cores were analyzed for particle size, agrichemicals, bulk sediment chemistry, bulk sediment density, total carbon, and isotopes (presented elsewhere, see Bennett and Rhoton, 2003).

2. Discrimination of post-impoundment sediment (sediment deposited since dam construction) and pre-impoundment sediment (parent material or pre-existing sediment) was accomplished by (a) the use of chemical isotopes and their geochronological interpretation, and (b) variations in sediment texture and bulk density with depth. Two sediment cores were analyzed for radioactive lead (^{210}Pb; 22-year half-life) and cesium (^{137}Cs; 30-year half-life) for the purpose of dating sediment horizons. The distributions of these isotopes were used to define the stratigraphic position of dam construction, i.e. 1954. Moreover, these timelines corresponded to depth variations in sediment texture and bulk density. That is, the post-impoundment sediments are enriched in clay (up to 80% by mass) and depleted in both silt (about 20% by mass) and sand (about 0% by mass) as compared to the parent or pre-impoundment materials.

3. A multi-frequency acoustic profiling system was used to image the post-impoundment sediments below the bottom of the lake. Using the results of the stratigraphic analysis presented above, there is very good agreement between the acoustically-determined horizons and the stratigraphically-determined post-impoundment sediment thickness. Sediment tends to be thicker in the topographic lows, or in this case the relict or drowned Yalobusha and Skuna River channels, as compared to the plateaus on either side representing the relict

floodplains. This suggests that the incised, relict channels are playing some role in concentrating, moving, and storing impounded sediment as a response to sediment deposition and normal operation of the reservoir.

4. Although there are small pockets of very thick sediment, >2 m, the impounded sediment in the arms of the Yalobusha and Skuna Rivers is about 0.5 to 1.0 m thick and about 1.5 m thick in the main pool of the lake. Sediment thickness tends to increase towards the pool region. This pattern of sedimentation is consistent with the stratigraphic results presented above.

5. The total volume of accumulated sediment based on these results is 40,357 ac-ft (49,790,128 m3), assuming that sediment thickness is zero at the lake shoreline. The as-built flood control storage is 1,251,710 ac-ft at a pool elevation of 231 ft. Using these values, the loss of flood control storage due to reservoir sedimentation since dam construction is approximately 3.3%. Thus, the reservoir has an annual storage loss of about 0.1%. These accumulation rates do not include sedimentation within the tributaries upstream of the lake and are restricted in space to those areas surveyed.

6. REFERENCES

Bennett, S.J., and F.E. Rhoton, 2003. Physical and chemical characteristics of sediment impounded within Grenada Lake, MS. USDA-ARS National Sedimentation Laboratory Research Report No. 36, 161pp.

Binford, M.W., and M. Brenner, 1986. Dilution of ^{210}Pb by organic sedimentation in lakes of different trophic states, and application to studies of sediment-water interactions. Limnology and Oceanography, 31, 584-595.

Downs, P.W., and A. Simon, 2001. Fluvial geomorphological analysis of the recruitment of large woody debris in the Yalobusha River network, Central Mississippi, USA. Geomorphology, 37, 65-91.

Dunbar, J.A., P.M. Allen, and P.D. Higley, 1999. Multifrequency acoustic profiling for water reservoir sedimentation studies. Journal of Sedimentary Research, 69, 521-527.

Lanesky, D.E., B.W. Logan, R.G. Brown, and A.C. Hine, 1979. A new approach to portable vibracoring underwater and on land. Journal of Sedimentary Petrology, 49, 654-657.

Ritchie, J.C., and J.R. McHenry, 1990. Application of radioactive fallout Cesium-137 for measuring soil erosion and sediment accumulation rates and patterns: A review. Journal of Environmental Quality, 19, 215-233.

Simon, A., 1998. Processes and forms of the Yalobusha River System: A detailed geomorphic evaluation. USDA-ARS National Sedimentation Laboratory Research Report 9, 131 pp.

Simon, A., and M. Rinaldi, 2000. Channel instability in the loess area of the Midwestern United States. Journal of the American Water Research Association, 36, 133-155.

Simon, A., and R.E. Thomas, 2002. Processes and forms of an unstable alluvial system with resistant, cohesive streambeds. Earth Surface Processes and Landforms, 27, 699-718.

Smith, D.G., 1984. Vibracoring fluvial and deltaic sediments: Tips on improving penetration and recovery. Journal of Sedimentary Petrology, 54, 660-663.